Organic & Biomolecular Chemistry

PAPER

View Article Online
View Journal

Cite this: DOI: 10.1039/c9ob00872a

Boosting the singlet oxygen photosensitization abilities of Zn(II) phthalocyanines through functionalization with bulky fluorinated substituents†

Miguel A. Revuelta-Maza,[a] Santi Nonell,[b] Gema de la Torre *[a,c] and Tomás Torres *[a,c,d]

Received 15th April 2019,
Accepted 11th July 2019

DOI: 10.1039/c9ob00872a

rsc.li/obc

In-depth, systematic photophysical studies have been performed on a series of **ABAB**, **A$_3$B** and **A$_4$** ZnPcs functionalized with a varying number of bis(trifluoromethyl)phenyl units (*i.e.* at the B isoindoles) and other electron-withdrawing/electron-donating moieties (*i.e.* at the A isoindoles), to determine the influence of the susbtitution pattern on the aggregation features, fluorescence quantum yields and singlet oxygen ($^1O_2$) generation abilities of these molecules. As a general trend, the larger the number of bis(trifluoromethyl)phenyl units (*i.e.* **ABAB** crosswise functionalized ZnPcs), the lower the fluorescence quantum yield and the higher the $^1O_2$ photosensitization. On the other hand, the electronic character of the substituents at the A isoindoles do not seem to have a clear effect on the photophysical properties of these **ABAB** ZnPcs. Overall, $^1O_2$ quantum yields determined by the direct observation of the $^1O_2$ phosphorescence are very high, with values ranging from 1 to 0.74 in THF solutions.

Introduction

Phthalocyanines (Pcs) represent the most prominent family of second-generation synthetic photosensitizers (PS),[1–4] mainly due to their strong absorption in the phototherapeutic window and the efficient sensitization of triplet oxygen ($^3O_2$) to form highly reactive singlet oxygen ($^1O_2$). Owing to their extended π-conjugation, Pcs exhibit a strong tendency to aggregate that drives the formation of oligomers in solution.[5] The formation of stacked aggregates affects their photochemical and photophysical properties, and hence their use as PS, because aggregation-induced fast radiationless deactivation detracts from $^1O_2$ generation. In aqueous media, aggregation of Pcs is facilitated by their inherent insolubility. In this context, hydrophilic groups can be introduced to render an amphiphilic character and water-solubility to the Pcs,[6–8] but they do not bring about the elimination of the aggregation tendency of Pcs in this medium. A means to circumvent the aggregation derived from the π–π stacking of Pcs arises from the complexation of closed shell, diamagnetic metal ions such as Si(IV)[6,9] or Ru(II),[10] which can be axially functionalized with the required hydrophilic moieties.

On the other hand, ZnPcs are very interesting PS as they present, in general, higher efficiencies in the generation of $^1O_2$ than the abovementioned Ru(IV)Pcs or Si(IV)Pcs.[11] However, an important shortcoming of ZnPcs is that they cannot circumvent the π–π stacking issues by covalent axial functionalization. In this regard, our research group has recently described a new strategy to prepare ZnPcs showing both hindered aggregation and water solubility, that is, by introducing two types of peripheral substituents into the Pc in a crosswise, **ABAB** architecture[12,13] (A and B coding for the two differently functionalized isoindole constituents). Within this architecture, π–π interactions between the Pc cores are prevented by endowing two facing isoindoles (B) of the ZnPc with bulky bis(trifluoromethyl)phenyl units, while the other two isoindoles (A) can provide the necessary water-solubility if they are properly functionalized with hydrophilic substituents. Interestingly, **ABAB** ZnPcs with extra-annulated phthalimide units containing different moieties in the nitrogen positions gave rise to $^1O_2$ quantum yields (ϕ_Δ) that are higher than the average values reported in the literature for other functionalized ZnPcs, which proved our **ABAB** ZnPcs to be very interesting motifs for the preparation of PS.[13]

[a]Universidad Autónoma de Madrid, c/Francisco Tomás y Valiente 7, 28049 Madrid, Spain. E-mail: tomás.torres@uam.es, gema.delatorre@uam.es
[b]Institut Químic de Sarrià, Universitat Ramon Llull, 08017 Barcelona, Spain
[c]Institute for Advanced Research in Chemical Sciences (IAdChem), Universidad Autónoma de Madrid, 28049 Madrid, Spain
[d]Instituto Madrileño de Estudios Avanzados (IMDEA)-Nanociencia, c/Faraday 9, Cantoblanco, 28049 Madrid, Spain

†Electronic supplementary information (ESI) available: Synthetic details and spectroscopic and photophysical characterization. See DOI: 10.1039/c9ob00872a

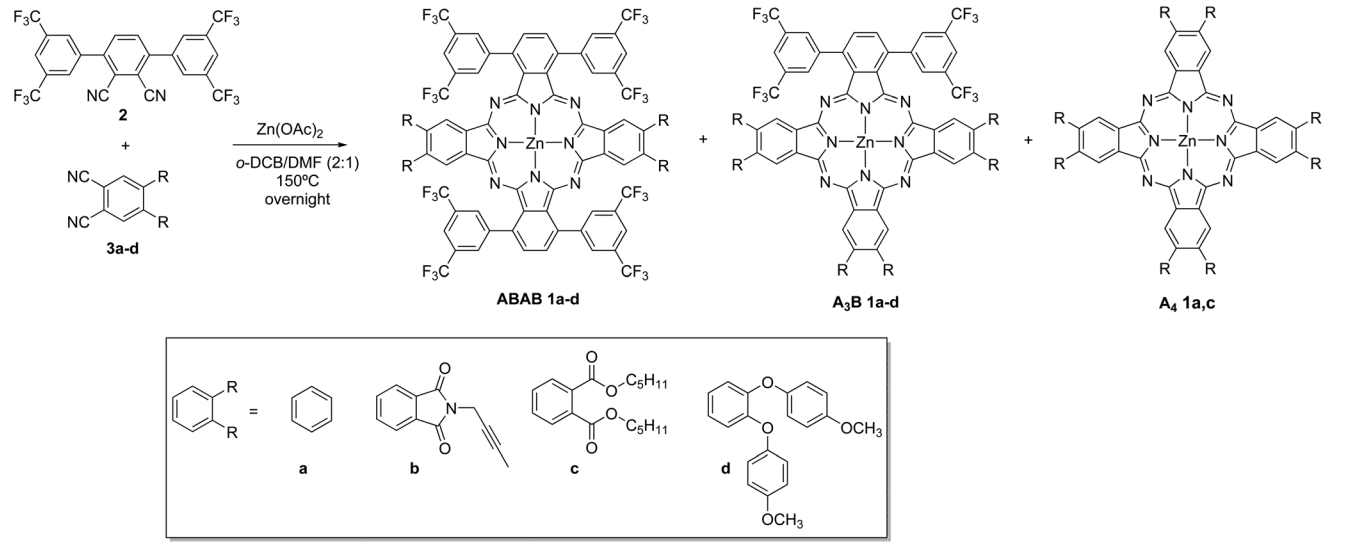

Scheme 1 Synthesis of ZnPcs **ABAB 1a–d**, A_3B **1a–d** and A_4 **1a,c**.

Before using this **ABAB** ZnPc skeleton to build amphiphilic, water-soluble chromophores with plausible application as PS, we have tackled an in-depth study to establish structure/activity relationships that can help us to design and prepare ZnPcs with maximized ϕ_Δ. From previous studies performed over different types of fluorinated Pcs,[14–18] and from our own results,[13] we can assume that the functionalization with bis(trifluoromethyl)phenyl units at the alpha position of the outer benzene rings of the Pc could be responsible for the high $^1O_2$ generation efficiencies found by us,[13] as a result of: (i) the position of the fluorinated substituents, since alpha-substitution is usually preferable *versus* beta functionalization at the ZnPc;[19] (ii) the enhanced photostability that fluorine-functionalization affords to the ZnPc,[20] due to the electron-withdrawing character of the CF_3 groups that results in energetically low-lying highest occupied molecular orbitals (HOMOs);[21] and/or the heavy atom effect that favors intersystem crossing and, therefore, high triplet lifetimes.[14–16]

Then, we aim here to verify the effect of the functionalization with bis(trifluoromethyl)phenyl units by preparing and studying the photophysical features of a series of ZnPcs endowed with a different number of fluorinated substituents (*i.e.* **ABAB 1a–d**, A_3B **1a–d** and A_4 **1a** and **c**) (Scheme 1). Moreover, to determine the effect that the nature of the substituents at the A isoindoles exerts on the electronic structure, and therefore, on the photophysical properties of the compounds, we have synthesized a series of ZnPcs with A units lacking any functional group (**1a** series), or endowed with either electron-withdrawing functional groups, such as extra-annulated phthalimides (**1b** series)[13] and ester moieties (**1c** series),[13] or electron-donating *p*-methoxyphenoxy substituents (**1d** series). Importantly, the functionalization incorporated into ZnPcs **ABAB 1b–d** would enable further chemical modifications to convert these series of compounds into real water-soluble molecules, with a balanced hydrophilicity/lipophilicity,[15,16] for their use as PS. Therefore, this systematic study would allow us to establish optimal ZnPc cores for the divergent preparation of a number of amphiphilic PS.

Results and discussion

Synthesis

The synthesis of the target ZnPcs was carried out by cross-condensation between equimolecular amounts of bulky phthalonitrile **2** (B) and phthalonitriles **3a–d** (A). In all the reactions, the corresponding ZnPcs **ABAB 1a–d** were formed, together with the related A_3B **1a–d** and A_4 **1a–d** derivatives. As previously observed in preceding studies,[12,13] no traces of Pcs with two adjacent B units were observed, due to the presence of rigid phenyl groups in the 3,6-positions of the corresponding phthalonitrile that hampers its self-condensation. All **ABAB** and A_3B derivatives were easily isolated by chromatographic means, in yields ranging from 2% to 9% for the **ABAB** series, and from 5% to 12% for the A_3B ZnPcs. In contrast, A_4-type compounds could not be isolated in appropriate quantities and purities, mainly due to their low solubility and their manifest aggregation tendency, with the exception of A_4 **1c**, which was isolated and characterized. For that reason, only A_4 **1c** and the commercially available A_4 **1a** (that is, non-functionalized ZnPc) could be included in the photophysical study.

Apart from the rather insoluble unsubstituted A_4 **1a**, the rest of the synthesized ZnPcs have in common good solubility features. This fact, together with the high symmetry exhibited by all the derivatives, results in extremely well-resolved ^{1}H- and ^{13}C NMR spectra (see the ESI†), which is infrequent for ZnPcs. As an example, the ^{1}H NMR spectra of compound **ABAB 1d** are shown in Fig. 1. The good resolution observed in the spectrum of A_3B **1a** is worth mentioning, which points out the ability of the bis(trifluoromethyl)phenyl moieties to hamper aggregation

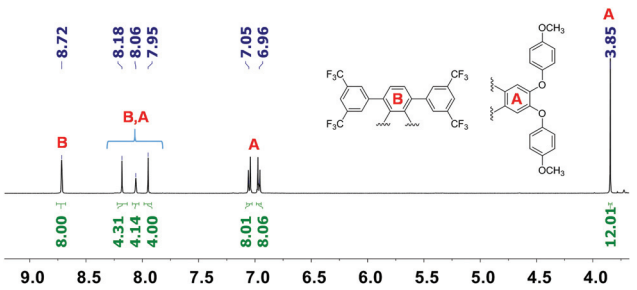

Fig. 1 ^{1}H NMR spectrum (500 MHz, THF-d_8) of ZnPc **ABAB 1d**.

in solution, even if only one isoindole is functionalized with these bulky groups. Geometry optimization of **ABAB 1a** and **A_3B 1a** structures performed with SCIGRESS (FJ 2.8.1 EU 3.3.1) well-illustrates how bis(trifluoromethyl)phenyl substituents hamper the stacking of the ZnPc macrocycles (see Fig. S1 in the ESI†).

Photophysical studies

First, ground-state absorption experiments were performed for all the ZnPcs, showing the typical Q band and B band transitions.[22] UV-vis absorption spectra were first recorded in THF, a solvent that is able to coordinate the Zn(II) metal centre, hampering the aggregation of ZnPcs independently of the substitution pattern. On the other hand, when the UV-vis experiments were performed in toluene, hints of aggregation were observed for **A_3B 1c** and **A_4 1c**, with Q bands featuring shoulders at longer wavelengths. Aggregation in toluene solutions of these compounds was further confirmed in concentration-dependent studies (see below). Importantly, in the case of non-functionalized ZnPc **A_4 1a**, the solutions in both THF and toluene had to be prepared from a stock solution in DMSO (1% final content), which also contributed to the disaggregation of the Pc.

As an example to visualize the absorption changes along the **ABAB**, **A_3B** and **A_4** series, the UV-vis spectra of all the members of the **1a** family are depicted in Fig. 2. The **ABAB** and **A_3B** derivatives show split Q bands both in toluene and THF, accompanied by the typical vibrational absorptions, although splitting is much more pronounced in **ABAB 1a**, which is consistent with its D_{2h} symmetry. Increasing the number of α-bis(trifluoromethyl)phenyl substituents produces a red-shift of the Q band maximum, namely, from 666 nm for **A_4 1a** to 698 nm for **ABAB 1a** in THF solutions (Table 1). The other three families (**1b–d**), with different types of substituents in the A isoindole units, showed similar behaviour when the different members of each family are compared, with the exception of the **1c** series, which show a single Q band in THF for the three **ABAB**, **A_3B** and **A_4** members (see Fig. 3 and the ESI†). The spectra of the **ABAB** members of the four series of ZnPcs **1a–d** are superimposed in Fig. 3a, and the same applies for the **A_3B** members in Fig. 3b. In both the **ABAB** and the **A_3B** series, ZnPcs **1d** with facing *N*-functionalized phthalimides display the largest red shift.

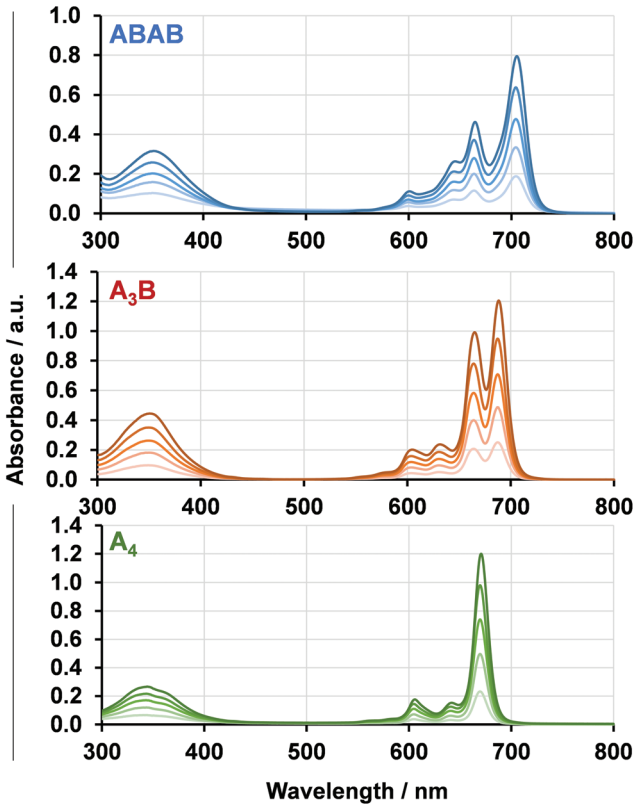

Fig. 2 Concentration-dependent UV-vis experiments for ZnPcs **1a** in THF (1×10^{-6}–9×10^{-6} M).

Table 1 Photophysical properties of ZnPcs **1a–d** in THF solution. Estimated uncertainties in the quantum yields are ±10%

ZnPc	log ε (λ)	λ_f/nm	ϕ_f	τ_S/ns	τ_T[a]/μs	ϕ_Δ
ABAB 1a	4.72 (348), 4.93 (662), 5.11 (698)[b]	705	0.05	1.7	0.32	~1
A_3B 1a	4.85 (347), 5.17 (677), 5.22 (682)[b]	686	0.11	2.5	0.18	0.92
A_4 1a[c]	4.54 (350), 5.17 (666)[b]	669	0.17	3.4	0.28	0.79
ABAB 1b	4.73 (349), 5.03 (676), 5.16 (712)[b]	717	0.06	2.1	0.13	0.74
A_3B 1b	4.73 (359), 5.10 (698)[b]	711	0.08	2.4	0.46	0.74
ABAB 1c	4.90 (350), 5.50 (687)[b]	693	0.08	3.0	0.23	0.80
A_3B 1c	4.87 (348), 5.46 (684)[b]	691	0.12	3.1	0.22	0.78
A_4 1c	4.49 (350), 5.05 (682)[b]	687	0.09	3.2	0.25	0.73
ABAB 1d	4.80 (358), 5.13 (671)[b], 5.15 (704)	711	0.06	1.8	0.27	0.86
A_3B1d	4.82 (358), 5.08 (674)[b], 5.15 (693)	695	0.09	2.1	0.17	0.84

[a] In air-saturated solutions. [b] Q-band maximum. [c] Prepared from a stock solution of the ZnPc in DMSO (final content: 1% DMSO).

From this initial comparison, a first conclusion arises regarding the merits of these compounds as PS. In principle, the red-shifted absorption of **ABAB** ZnPcs is an advantage for photodynamic therapy, which, together with their wider range of absorption wavelengths (*i.e.* covering approximately 190 nm, while only 140 nm for **A_4** derivatives), render **ABAB** compounds more outstanding than their counterparts.

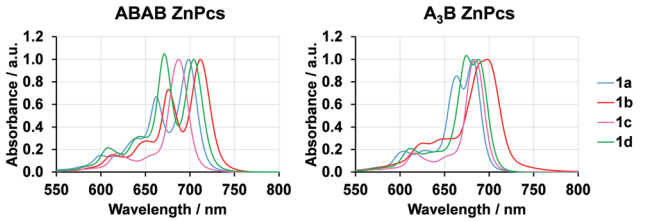

Fig. 3 UV-vis spectra for **ABAB 1a–d** and **A_3B 1a–d** in THF (Q-band normalized).

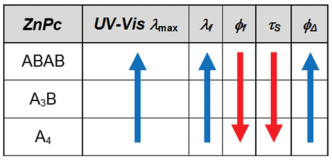

Fig. 5 Trends observed in the photophysical properties for each family of ZnPcs **1a–d**.

The lack of aggregation in THF and toluene solutions for most of these ZnPcs was proven by the absorption studies performed in a range of concentrations (Fig. 2 and Fig. S17–S25†). For the verification of the Lambert–Beer law, an analysis of linear regression between the intensity of the Q-band and the concentration of the ZnPcs was performed. Under the conditions of our concentration-dependent studies, only **A_3B 1c** and **A_4 1c** showed aggregation evidence in toluene solutions (namely, the linear fitting in this solvent does not pass through the origin of coordinates, see Fig. S22†) thus confirming our previous assumption. Further demonstration was achieved upon the addition of 1% THF over the solutions of the two compounds in toluene. The spectra recorded in the presence of the coordinative solvent showed relevant changes in the form of a single Q band with no traces of the red-shifted shoulder (Fig. S23†). Also in ^{1}H NMR experiments, the addition of 1% THF-d_6 over a toluene-d_8 solution improves the resolution of the aromatic signals (Fig. S11†). The fact that **A_3B-1c** is the only compound of the **A_3B** series displaying aggregation, can be rationalized on the basis of the presence of ester functions, which can coordinate the Zn (II) centre of a vicinal ZnPc to give *J*-type aggregates (Fig. S11b†).[5,23]

Fluorescence experiments (Fig. 4a) are in line with absorption assays: a shift to longer wavelengths takes place when increasing the number of bis(trifluoromethyl)phenyl units over the Pc core. In contrast, fluorescence quantum yields (ϕ_f) increase in the opposite direction, (*i.e.* ϕ_f: **A_4-** > **A_3B-** > **ABAB-**derivatives) (Fig. 5, Table 1 and Table S1 in the ESI†).

Also, the quantification of the ϕ_Δ was performed for these series of compounds, by direct observation of the $^1O_2$ phosphorescence at 1275 nm after excitation at 355 nm, both in THF and toluene solutions (see Fig. 4b, Table 1 and Table S1†). Regardless of the solvent, the same trend was observed for the four families of compounds, namely, an increase of the ϕ_Δ takes place when adding bis(trifluoromethyl)phenyl units to the ZnPc core (*i.e.* **A_4-** < **A_3B-** < **ABAB-**derivatives) concomitantly with a ϕ_f decrease, as depicted in Fig. 5 for the **ABAB 1a**, **A_3B 1a** and **A_4 1a** series. Also, time-resolved fluorescence decays pointed in the same direction (Fig. S36–S39†), showing singlet excited-state lifetimes decreasing from **A_4** to **ABAB** ZnPcs. These observations support our previous findings[13] that pointed to the alpha-substitution with these fluorinated aromatic groups as the driving force that pushes up $^1O_2$ generation abilities of ZnPcs.

On the other hand, the impact of the substitution in the A isoindole on the photosensitization abilities of the ZnPc has been also analyzed. The first remark concerns the very high ϕ_Δ values observed in the **1a** series, lacking functionalization in the A isoindole, especially that of **ABAB 1a**, which is very close to 1 in THF (see Table 1). Beyond this remarkable value, when one compares the other three substituted **ABAB** derivatives, ϕ_Δ values in THF are all between 0.86 and 0.74, which are still far above average. In THF, the ϕ_Δ of the **ABAB** series follows the trend **1a** > **1d** > **1c** > **1b**. However, in toluene solutions (see Table S1†), all the ϕ_Δ values of the **ABAB** ZnPcs decrease in comparison with those in THF, and vary in the **1a** > **1c** > **1b** > **1d** direction, ranging from 0.76 for **ABAB 1a** to 0.62 for **ABAB 1d**. These results point to a minor impact of the substitution at the A isoindole on the photophysical properties of the analysed ZnPc derivatives.

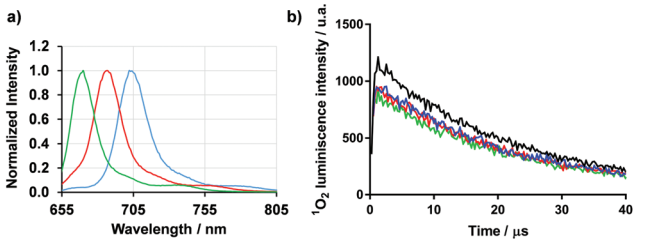

Fig. 4 (a) Fluorescence spectra of ZnPcs **1a** and (b) $^1O_2$ production of ZnPcs **1c** against phenalenone (black line) for **ABAB** ZnPcs (blue lines), **A_3B** ZnPcs (red lines) and **A_4** ZnPcs (green lines) in THF.

Conclusions

The study of a number of ZnPcs with an iterating substitution pattern, that is, a varying number of B isoindoles containing bis(trifluoromethyl)phenyl substituents (*i.e.* **ABAB-**, **A_3B-** and **A_4-1** series), and with different functionalization in the A isoindole (*i.e.* **1a–d** series), has allowed us to ascertain the determinant role of the bulky, fluorinated substituents in the photophysical properties and $^1O_2$ generation capabilities of these compounds. For all the **1a–d** series, the **ABAB** substitution provides the ZnPcs with the most red-shifted absorptions and non-aggregating features that are independent of the solvent employed, as well as the highest $^1O_2$ quantum yields. These are outstanding characteristics, not easy to gather in ZnPcs,

and that are all fundamental for using them as PS in therapeutic applications. Remarkable data found in these studies are the ϕ_Δ close to 1 obtained for compound **ABAB 1a**, with no functionalization at the A isoindoles, which evidences the relevant function of bis(trifluoromethyl)phenyl moieties on the $^1O_2$ production. On the other hand, adding substituents at the A isoindole produces a slightly detrimental effect on the ϕ_Δ, although the values are still very high, above the average of the figures of merit reported for ZnPc photosensitizers. We did not find a clear relationship between the electronic character of the substituents at the A isoindole and the $^1O_2$ production, since the trends change with the solvent employed. However, **ABAB 1d** is, with its ϕ_Δ of 0.86 in polar THF, a candidate of choice for further derivatization of the four phenolic positions with hydrophilic substituents in the search for efficient PS, considering also that **ABAB 1d** is the compound of the **ABAB** series that was isolated in better chemical yield.

Therefore, our rational study will allow us to develop efficient **ABAB** ZnPc derivatives with balanced hydrophilicity and lipophilicity, in the search of non-aggregated chromophores, soluble in water media and with high ϕ_Δ, which can find application in photodynamic therapies.

Experimental section

General information

Chemicals were purchased from commercial suppliers and used without further purification unless stated otherwise. 3,3″,5,5″-tetrakis(trifluoromethyl)-[1,1′:4′,1″-terphenyl]-2′,3′-dicarbonitrile (**2**),[12a] 2-(but-2-yn-1-yl)-1,3-dioxoisoindoline-5,6-dicarbonitrile (**3b**),[13] dipentyl 4,5-dicyanophthalate (**3c**),[24] and 4,5-bis(4-methoxyphenoxy)phthalonitrile (**3d**)[25] have been prepared according to published procedures. The monitoring of the reactions was carried out by thin layer chromatography (TLC), employing aluminum sheets coated with silica gel type 60 F254 (0.2 mm thick, E. Merck). Purification and separation of the synthesized products were performed by column chromatography, using silica gel (230–400 mesh, 0.040–0.063 mm, Merck). Eluents and relative proportions of the solvents are indicated for each particular case. Size exclusion chromatography was performed using a Bio-Beads S-X1 (200–400 mesh, Bio-Rad). Infrared (IR) spectra were recorded on an Agilent Technologies Cary 630 FTIR spectrophotometer, employing in all cases solid samples (diamond ATR). Mass Spectrometry (MS) and High Resolution Mass Spectrometry (HRMS) spectra were recorded employing Matrix Assisted Laser Desorption/Ionization-Time of Flight (MALDI-TOF), using a Bruker Reflex III spectrometer, with a nitrogen laser operating at 337 nm. The different matrixes employed are indicated for each spectrum. Mass spectrometry data are expressed in *m*/*z* units. NMR spectra (^{1}H NMR, ^{13}C NMR) were recorded on a Bruker AC-300 (300 MHz) instrument or a Bruker XRD-500 (500 MHz). ^{13}C NMR spectra for **A$_3$B**-ZnPcs are not detailed due to the great complexity and high number of overlapped signals.

General procedure for the synthesis of ZnPcs 1a–d

2 (0.27 mmol, 150 mg), phthalonitrile **3a–d** (0.27 mmol) and anhydrous $Zn(AcO)_2$ (0.27 mmol, 50 mg) were placed in a 5 mL high pressure resistant flask equipped with a magnetic stirrer, and then 2.7 mL ([**2**] = 0.1 M) of dry *o*-dichlorobenzene/DMF (dried over 4 Å molecular sieves) 2 : 1 were added. The mixture was heated to 150–160 °C overnight under an argon atmosphere. After cooling, the solvent was removed under vacuum. The mixture of products was purified by column chromatography on SiO_2.

Synthesis of ZnPcs 1a. Column chromatography on SiO_2 (dioxane/heptane in gradient from 1 : 4 to 1 : 2) was performed. The first fraction to elute contained the desired product **ABAB**, followed by compound **A$_3$B**. Non-functionalized ZnPc (**A$_4$ 1a**) is commercially available.

ABAB 1a. The product was further purified by additional column chromatography on Bio-Beads using $CHCl_3$ as the eluent. After evaporation of the solvent, a blue solid was obtained, which was washed with MeOH. Yield: 15.2 mg, (8%). IR (ATR) ν^{-1} (cm^{-1}): 1374 (pyrrole ring), 1273 (C–F st), 1167 (C–F st), 1123, 896, 838; ^{1}H NMR (500 MHz, acetone-d$_6$): δ 8.00 (br s, 4H, HAr), 8.28 (br s, 4H, HAr), 8.35 (s, 4H, HAr), 8.62 (s, 4H, HAr), 8.89 (s, 4H, HAr); ^{13}C NMR (125 MHz, acetone-d$_6$): δ 122.7 (C Ar), 123.2 (C Ar), 125.0 (q, J = 275.5 Hz, CF_3), 130.2 (C Ar), 132.0 (br s, C*CF_3), 132.3 (C Ar), 132.7 (C Ar), 136.3 (CH Ar), 137.7 (CH Ar), 139.3 (CH Ar), 144.2 (CH Ar), 153.4 (C═N), 154.4 (C═N); HR-MS (MALDI ULTRAFLEX, matrix DCTB + PPG1000 + 2000): *m*/*z* 1424.1019 (calculated for $C_{64}H_{24}F_{24}N_8Zn$: 1424.1027).

A$_3$B 1a. The product was further purified by additional column chromatography on Bio-Beads using THF as the eluent. After evaporation of the solvent a blue solid was obtained, which was washed with MeOH. Yield: 10.1 mg, (11%). IR (ATR) ν^{-1} (cm^{-1}): 1376 (pyrrole ring), 1332 (C–F st), 1271 (C–F st), 1119, 893, 830; ^{1}H NMR (500 MHz, THF-d$_8$): δ 7.95–8.02 (m, 2H, HAr), 8.06–8.16 (m, 4H, HAr), 8.21 (s, 2H, HAr), 8.31 (d, J = 7.37 Hz, 2H, HAr), 8.60 (s, 2H, HAr), 8.90 (s, 4H, HAr), 9.27–9.35 (m, 4H, HAr); HR-MS (MALDI ULTRAFLEX III, matrix DCTB + PPG1000): *m*/*z* 1000.0900 (calculated for $C_{48}H_{20}F_{12}N_8Zn$: 1000.0905).

Synthesis of ZnPcs 1b. Column chromatography on SiO_2 (THF/heptane in gradient from 2 : 1 to 1 : 1) was performed. The first fraction to elute contained the desired product **ABAB** followed by compounds **A$_3$B** and **A$_4$**. **ABAB 1b** had been previously synthesized and characterized.[13]

A$_3$B 1b. The product was further purified by additional column chromatography on Bio-Beads using $CHCl_3$ as the eluent. After evaporation of the solvent a blue-green solid was obtained, which was washed with heptane. Yield: 6.3 mg, (5%). IR (ATR) ν^{-1} (cm^{-1}): 2914, 2845, 2301 (C≡C st), 1769 (C═O st), 1717, 1421, 1379 (CH_3 δ sim), 1341 (C–F st), 1211 (C–F st), 1165, 1126; ^{1}H NMR (300 MHz, DMSO-d$_6$): δ 1.86–2.06 (m, 9H, CH_3), 4.58–4.83 (m, 6H, CH_2), 8.21–8.66 (m, 6H, CHAr), 8.79 (br s, 4H, CHAr), 8.87–9.32 (m, 4H, CHAr); HR-MS (MALDI ULTRAFLEX III, matrix DCTB + PPGNa 1000 + PPGNa

2000): *m*/*z* 1363.1356 (calculated for $C_{66}H_{29}F_{12}N_{11}O_6Zn$: 1363.1397).

A_4 1b. MS (MALDI, matrix DCTB): *m*/*z* 1060.3 (calculated for $C_{56}H_{28}N_{12}O_8Zn$: 1060.1).

Synthesis of ZnPcs 1c. Column chromatography on SiO_2 (THF/heptane in gradient from 1 : 4 to 1 : 1). The first fraction to elute contained the desired product **ABAB** followed by compounds **A_3B** and **A_4**. **ABAB 1c** [13] and **A_4 1c** [26] had been previously synthesized and characterized.

A_3B 1c. The product was further purified by additional column chromatography on Bio-Beads using $CHCl_3$ as the eluent. After evaporation of the solvent a blue solid was obtained, which was washed with MeOH. Yield: 18.5 mg, (12%). IR (ATR) ν^{-1} (cm^{-1}): 2954, 2928, 2858, 1718 (C═O st), 1464, 1377, 1334, 1263 (C–F st), 1172 (C–F st), 1127, 1091 (C–O st); ^{1}H NMR (300 MHz, acetone-d_6): δ 0.97–1.17 (m, 18H, CH_3), 1.47–1.71 (m, 24H, CH_2), 2.67–2.87 (m, 12H, CH_2), 4.47–4.73 (m, 12H, CH_2), 8.40 (s, 2H, CHAr), 8.50 (s, 2H, CHAr), 8.63 (s, 2H, CHAr), 8.97 (s, 4H, CHAr), 9.38 (s, 2H, CHAr), 9.49 (s, 2H, CHAr); HR-MS (MALDI ULTRAFLEX III, matrix DCTB + PPG1000 + 2000): *m*/*z* 1684.5043 (calculated for $C_{84}H_{80}F_{12}N_8O_{12}Zn$: 1684.4990).

Synthesis of ZnPcs 1d. Column chromatography on SiO_2 (heptane/EtOAc 1 : 1 as the eluent) was performed. The first fraction to elute contained the desired product **ABAB**, followed by compounds **A_3B** and **A_4**.

ABAB 1d. The product was further purified by additional column chromatography on Bio-Beads using $CHCl_3$ as the eluent. After evaporation of the solvent a blue solid was obtained, which was washed with MeOH. Yield: 23 mg (9%). IR (ATR) ν^{-1} (cm^{-1}): 2925 (ar, C–H st), 1502, 1410, 1376 (pyrrole ring), 1276 (C–O–C st as), 1198 (C–F st), 1177 (C–F st), 1133; ^{1}H NMR (300 MHz, DMSO-d6): δ 3.8 (s, 12H, OMe), 7.03 (d, *J* = 9.10 Hz, 8H, O–Ph–O), 7.12 (d, *J* = 9.10 Hz, 8H, O–Ph–O), 7.76 (s, 4H, CHAr), 7.99 (s, 4H, CHAr), 8.25 (s, 4H, CHAr), 8.78 (s, 8H, CHAr); ^{1}H NMR (500 MHz, THF-d8): δ 3.8 (s, 12H, OMe), 6.96 (d, *J* = 9.18 Hz, 8H, O–Ph–O), 7.05 (d, *J* = 9.18 Hz, 8H, O–Ph–O), 7.95 (s, 4H, CHAr), 8.06 (s, 4H, CHAr), 8.18 (s, 4H, CHAr), 8.72 (s, 8H, CHAr); ^{13}C NMR (125 MHz, THF-d_8): δ 55.7 (CH_3), 115.5 (CHAr PhOMe), 115.7 (CHAr), 119.4 (CHAr PhOMe), 122.4 (C Ar), 126.8 (q, *J* = 273.6 Hz, CF_3), 131.9 (br s, C*CF_3), 132.0 (C Ar), 132.2 (C Ar), 132.6 (C Ar), 135.6 (CH Ar), 136.2 (CH Ar), 137.9 (CH Ar), 144.0, 152.3, 152.9, 153.3, 154.0, 156.9 (C Ar); HR-MS (MALDI ULTRAFLEX III, matrix: DCTB): *m*/*z* 1912.2488 (calculated for $C_{92}H_{48}F_{24}N_8O_8Zn$: 1912.2498).

A_3B 1d. The product was further purified by additional column chromatography on Bio-Beads using $CHCl_3$ as the eluent. After evaporation of the solvent a blue solid was obtained, which was washed with MeOH. Yield: 9.4 mg (6%). IR (ATR) ν^{-1} (cm^{-1}): 2954 (ar, C–H st), 2883 (ar, C–H st), 1723, 1507, 1449, 1362 (pyrrole ring), 1279 (C–O–C st as), 1182 (C–F st), 1134 (C–F st), 1034; ^{1}H NMR (300 MHz, DMSO-d6): δ 3.81 (s, 6H, OMe), 3.82 (s, 6H, OMe), 3.83 (s, 6H, OMe), 6.97–7.08 (m, 8H, O–Ph–O), 7.10–7.17 (m, 8H, O–Ph–O), 7.17–7.28 (m, 8H, O–Ph–O), 7.77 (s, 2H, CHAr), 8.00 (s, 2H, CHAr), 8.22 (s, 2H, CHAr), 8.54 (s, 2H, CHAr), 8.59 (s, 2H, CHAr), 8.78 (s, 4H, CHAr); HR-MS (MALDI ULTRAFLEX III, matrix: DCTB): *m*/*z* 1732.3115 (calculated for $C_{90}H_{56}F_{12}N_8O_{12}Zn$: 1732.3112).

A_4 1d. HR-MS (MALDI ULTRAFLEX III, matrix DCTB + PEGNa 1500): *m*/*z* 1552.3741 (calculated for $C_{88}H_{64}N_8O_{16}Zn$: 1552.3726).

Conflicts of interest

There are no conflicts to declare.

Acknowledgements

This work was supported by MINECO (CTQ2017-85393-P and CTQ2016-78454-C2-1-R) and ERA-NET/MINECO EuroNanoMed2017-191/PCIN-2017-042.

Notes and references

1 V. V. Roznyatovskiy, C.-H. Lee and J. L. Sessler, *Chem. Soc. Rev.*, 2013, **42**, 1921.
2 H. Lu and N. Kobayashi, *Chem. Rev.*, 2016, **116**, 6184.
3 T. Basova, A. Hassan, M. Durmus, A. G. Gürek and V. Ahsen, *Coord. Chem. Rev.*, 2016, **310**, 131.
4 V. Almeida-Marrero, E. van de Winckel, E. Anaya-Plaza, T. Torres and A. de la Escosura, *Chem. Soc. Rev.*, 2018, **47**, 7369.
5 X. F. Zhang, Q. Xi and J. Zhao, *J. Mater. Chem.*, 2010, **20**, 6726.
6 E. van de Winckel, B. David, M. M. Simoni, J. A. González-Delgado, A. de la Escosura, Â. Cunha and T. Torres, *Dyes Pigm.*, 2017, **145**, 239.
7 Y. Li, J. Wang, X. Zhang, W. Guo, F. Li, M. Yu, X. Kong, W. Wu and Z. Hong, *Org. Biomol. Chem.*, 2015, **13**, 7681.
8 V. Koç, S. Z. Topal, D. Aydın Tekdaş, Ö. D. Ateş, E. Önal, F. Dumoulin, A. G. Gürek and V. Ahsen, *New J. Chem.*, 2017, **41**, 10027.
9 M. Bispo, P. M. R. Pereira, F. Setaro, M. S. Rodríguez-Morgade, R. Fernandes, T. Torres and J. P. C. Tomé, *ChemPlusChem*, 2018, **83**, 855; E. van de Winckel, R. J. Schneider, A. de la Escosura and T. Torres, *Chem. – Eur. J.*, 2015, **21**, 1855.
10 J. T. Ferreira, J. Pina, C. A. F. Ribeiro, R. Fernandes, J. P. C. Tome, M. S. Rodriguez-Morgade and T. Torres, *ChemPhotoChem*, 2018, **2**, 640; J. T. Ferreira, J. Pina, C. A. F. Ribeiro, R. Fernandes, J. P. C. Tome, M. S. Rodriguez-Morgade and T. Torres, *J. Mater. Chem. B*, 2017, **5**, 5862.
11 X. Li, B.-D. Zheng, X.-H. Peng, S.-Z. Li, J.-W. Ying, Y. Zhao, J.-D. Huang and J. Yoon, *Coord. Chem. Rev.*, 2019, **379**, 147.
12 (*a*) E. Fazio, J. Jaramillo-García, G. de la Torre and T. Torres, *Org. Lett.*, 2014, **16**, 4706; (*b*) E. Fazio, J. Jaramillo-García, M. Medel, M. Urbani, M. Grätzel, M. K. Nazeeruddin, G. de la Torre and T. Torres, *ChemistryOpen*, 2017, **6**, 121.

13 M. A. Revuelta-Maza, C. Hally, S. Nonell, G. de la Torre and T. Torres, *ChemPlusChem*, 2019, **84**, 673–679.
14 A. Erdogmus and T. Nyokong, *Dyes Pigm.*, 2010, **86**, 174–181.
15 B. Pucelik, I. Gürol, V. Ahsen, F. Dumoulin and J. M. Dabrowski, *Eur. J. Med. Chem.*, 2016, **124**, 284–298.
16 K. Oda, S. Ogura and I. Okura, *J. Photochem. Photobiol., B*, 2000, **59**, 20–25.
17 A. Erdogmus and M. Arıcı, *J. Fluorine Chem.*, 2014, **166**, 127–133.
18 A. Erdogmus, S. Moenoa, C. Litwinskia and T. Nyokong, *J. Photochem. Photobiol., A*, 2010, **210**, 200–208.
19 B. G. Ongarora, X. Hu, H. Li, F. R. Fronczek and M. G. H. Vicente, *MedChemComm*, 2012, **3**, 179.
20 N. V. S. D. K. Bhupathiraju, W. Rizvi, J. D. Batteasb and C. M. Drain, *Org. Biomol. Chem.*, 2016, **14**, 389.
21 T. Furuyama, Y. Miyaji, K. Maeda, H. Maeda and M. Segi, *Chem. – Eur. J.*, 2019, **25**, 1678.
22 A. Günsela, E. Güzela, A. T. Bilgiçlia, G. Y. Atmacab, A. Erdoğmuşb and M. N. Yarasir, *J. Lumin.*, 2017, **192**, 888–892.
23 In spite of the lack of hydrophilicity of the reported ZnPcs, we have performed octanol/water partition experiments with the **ABAB-1c**, **A_3B-1c** and **A_4-1c** series of ZnPcs (see the ESI†). As expected, the ZnPcs were spectroscopically detected only in the octanol (water-saturated) phase. For the three ZnPcs, we observed a decrease in the Q-band maximum with respect to the absorption registered in dry 1-octanol at the same concentrations, probably due to precipitation/aggregation phenomena. The epsilon variation at the Q band maximum follows the sequence: **A_4-1c** (34%) > **A_3B-1c** (28%) > **ABAB-1c** (10%), which is in line with the aggregation behaviour of the three compounds. This result points out to a good solubilization in tissues of further amphiphilic **ABAB**-ZnPc derivatives from the water media.
24 B. Tylleman, R. Gómez-Aspe, G. Gbabode, Y. H. Geerts and S. Sergeyev, *Tetrahedron*, 2008, **64**, 4155.
25 M. Yoshioka, K. Ohta and M. Yasutake, *RSC Adv.*, 2015, **5**, 13828.
26 D. M. Opris, F. Nüesch, C. Löwe, M. Molberg and M. Nagel, *Chem. Mater.*, 2008, **20**, 6889.